ARTICLE

Extraordinarily High Efficiency Improvement for OLEDs with High Surface-Charge Polymeric Nanodots

Jwo-Huei Jou,[†,*] Wei-Ben Wang,[†] Mao-Feng Hsu,[†] Jing-Jong Shyue,[‡,*] Chuan-Huan Chiu,[†] I-Ming Lai,[†] Sun-Zen Chen,[§] Po-Hsien Wu,[†] Cheng-Chung Chen,[†] Chi-Ping Liu,[†] and Shih-Ming Shen[†]

[†]Department of Materials Science and Engineering, National Tsing Hua University, Hsin-Chu, Taiwan 30013, [‡]Research Center for Applied Sciences, Academia Sinica, Taipei, Taiwan 11529, and [§]Center for Nanotechology, Materials Science, and Microsystems, National Tsing Hua University, Hsin-Chu, Taiwan 30013

ABSTRACT The efficiency of highly efficient blue, green, red, and white organic light-emitting diodes (OLEDs) has been substantially advanced through the use of high surface-charge nanodots embedded in a nonemissive layer. For example, the blue OLED's markedly high initial power efficiency of 18.0 lm W^{-1} at 100 cd m^{-2} was doubled to 35.8 lm W^{-1} when an amino-functionalized polymeric nanodot was employed. At high luminance, such as 1000 cd m^{-2} used for illumination applications, the efficiency was improved from 12.4 to 21.2 lm W^{-1}, showing a significant enhancement of 71%. The incorporated highly charged nanodots are capable of effectively modulating the transportation of holes *via* a blocking or trapping mechanism, preventing excessive holes from entering the emissive layer and the resulting carrier-injection imbalance. Furthermore, in the presence of a high-repelling or dragging field arising from the highly charged nanodots, only those holes with sufficient energy are able to overcome the included barriers, causing them to penetrate deeper into the emissive layer. This penetration leads to carrier recombination over a wider region and results in a brighter emission and, therefore, higher efficiency.

KEYWORDS: organic light-emitting diode · nanodot · efficiency · surface charge · blue · white

*Address correspondence to jjou@mx.nthu.edu.tw, shyue@gate.sinica.edu.tw.

Received for review November 5, 2009 and accepted June 14, 2010.

Published online June 24, 2010. 10.1021/nn100357m

Polymeric nanodots (PNDs) are effective in improving the device efficiency of organic light-emitting diodes that are suitable for high-quality displays and area illumination.[1−4] In contrast to electrically neutral quantum dots and nanodots used in dry processes, polymeric nanodots can be synthesized with a precisely controlled size and wet-processed on soft substrates. This benefit from polymeric nanodots enables the realization of the large-area, roll-to-roll fabrication of flexible displays and lighting devices.[5−10] To replace current display technologies and illumination measures, such as incandescent bulbs and fluorescent tubes, the existing nanodots can be modified to improve their carrier-modulation capability and produce higher device efficiency.[10−17] Here we demonstrate a general method that substantially advances the efficiency of highly efficient organic light-emitting diodes (OLEDs) of all emissive colors, including white, *via* the incorporation of highly charged polymeric nanodots that are capable of modulating the transport flux of holes in the hole-injection layer effectively. One such example is the blue OLED, which has an initially high power efficiency of 18.0 lm W^{-1} at 100 cd m^{-2};[18] the efficiency of the blue OLED was doubled to 35.8 lm W^{-1} when an amino-functionalized PND was employed. This substantial advance in power efficiency offers a great potential for OLED displays to become a more competitive display, offering better energy saving, longer stand-by time, and even the most desired longer lifetime characteristics.

Previous studies on the deposition of quantum dots in the emissive layer or the incorporation of nanodots in the nonemissive layer have shown significant efficiency improvements for low-efficiency devices;[10−17] however, no report has yet revealed these approaches to be effective on high-efficiency devices, seriously limiting their practical applicability. The low electroluminescence (EL) efficiency may be attributed to a number of causes, including a high carrier-injection barrier,[4,10−12,17,20−23,26,27] poor carrier and exciton confinement,[10,11,22−27] exciton forming on guest molecules,[25,28,29] poor energy-transfer efficiency,[10−12,23−27] exciton quenching on guest molecules,[10,22−25] intrinsically low material electroluminescence,[10,19,23,30] and, most critically, imbalanced carrier injection,[4,10−12,17,19−23,27] which frequently leads to a poor recombination probability due to the excessive injection of holes or electrons. A recent work incorporating small polymeric nanodots in the nonemissive layer showed a 350% efficiency improvement for a white OLED with a power efficiency of 6.8 lm W^{-1};[11] however, the overall efficiency was still low even though the relative improvement was striking.

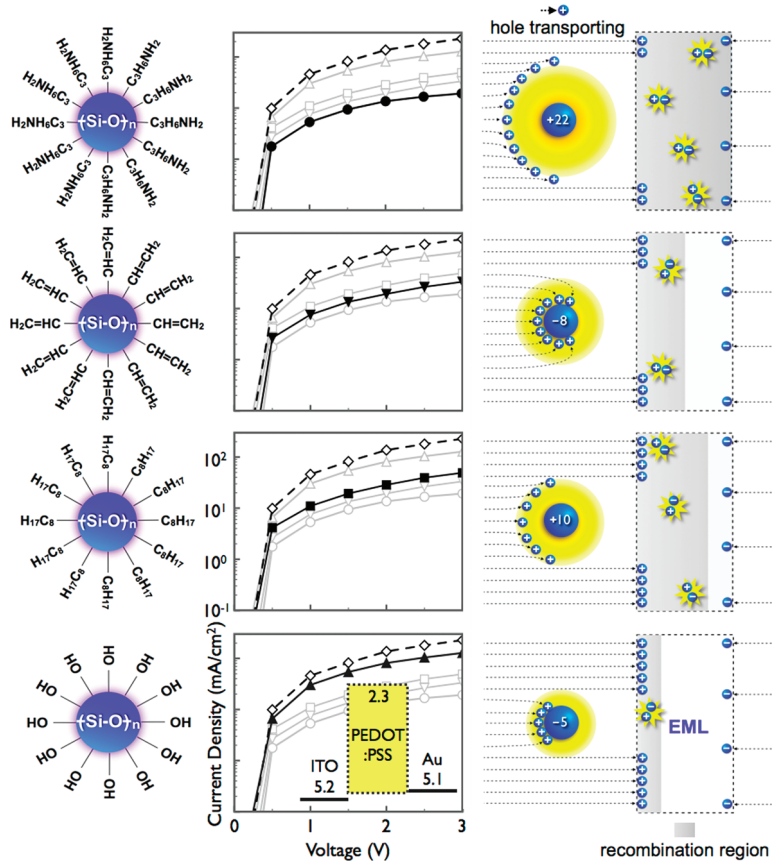

Figure 1. (Left) Schematic illustration of the structures of the four different PNDs studied: Am-PND, V-PND, Al-PND, and H-PND. (Middle) Incorporation effects of different PNDs at 0.7 wt % on the current density of a hole-transporting-only device consisting of a hole-injection layer of PEDOT:PSS sandwiched by a high work-function electrode pair. Devices with (●) Am-PND, (▼) V-PND, (□) Al-PND, (△) H-PND, and (◇) without any PND. The Am-PND device showed the lowest current density, implying that its highest positive charge was capable of most effectively repelling the injection of holes due to a strong repulsive effect and, consequently, small hole-transport flux. (Right) Schematic illustration of the plausible effects of charge intensity of the PNDs on the hole-transport flux, width of recombination region, and exciton population in the emissive layer.

In this report, we present the first use of small polymeric (polysilic acid) nanodots with a high surface charge, either negative or positive, to markedly enhance the efficiency of high-efficiency monochromatic or white OLEDs. For the most crucial blue emission, the incorporation of an amino-functionalized PND resulted in a power efficiency of 35.8 lm W^{-1} at 100 cd m^{-2}, a 99% improvement over the initially near-record-high efficiency of 18.0 lm W^{-1}.[18] Furthermore, at a high luminance, such as 1000 cd m^{-2}, the efficiency was enhanced from 12.4 to 21.2 lm W^{-1}, a marked enhancement of 71%. Most importantly, the incorporated concentration of PNDs required is so small that all of the original outstanding EL characteristics are largely unaffected, while the modulation of the hole transport flux is very effective in balancing the injection of holes against electrons. These results ensure that the present method will be effective for other high-efficiency OLEDs, as shown by the marked efficiency improvements from green, red, and white devices reported herein, whose power efficiencies at 100 cd m^{-2} were increased from 18.5 to 29.1, 1.6 to 2.1, and 17.1 to 26.3 lm W^{-1}, respectively.

RESULTS AND DISCUSSION

Figure 1 (left) is a schematic of the structure of the amino-functionalized PND (Am-PND) that possesses the highest ζ-potential (+22 mV) in THF relative to V-PND (−8 mV), Al-PND (+10 mV), and H-PND (−5 mV), which are modified by vinyl, alkyl, and hydroxyl functional groups, respectively. The sizes of the employed PND particles have been kept as close as possible; they are 9, 8, 7, and 8 nm for Am-PND, V-PND, Al-PND, and H-PND, respectively. While it is not possible to determine the amount of surface charge on the modified PND in a solid-state organic film, the ζ-potential of these PNDs in an organic solution was used to reflect their charge density and electric field in the organic film. In addition, because of the inevitable residual water in these polar environments, the surface charge gained from the hydrolysis (and/or acid−base) reaction would be retained upon drying. For H-PND, the surface Si−OH readily deprotonates; therefore, it possesses a negative charge. As a base, the amine group is protonated, and thus Am-PND has a positive potential. For Al-PND, because the alkane group is nonreactive, the positive charge may arise from the proton-

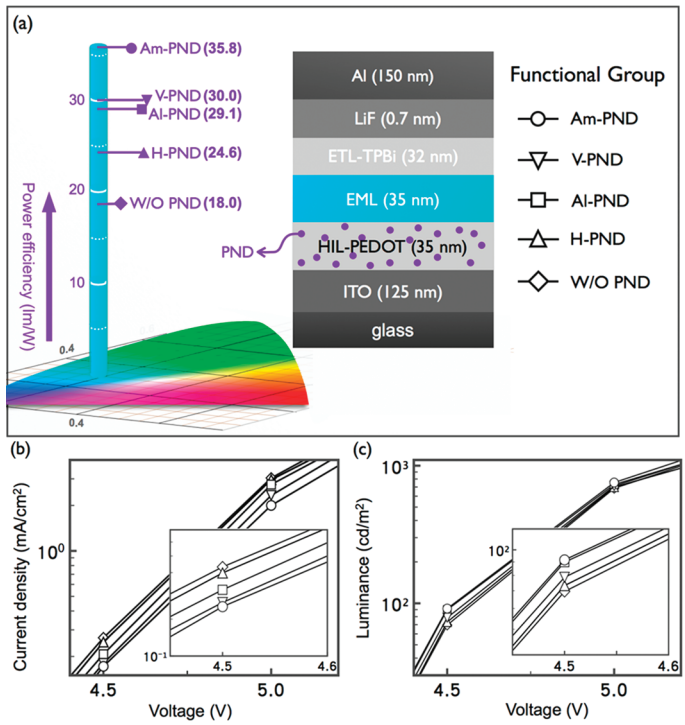

Figure 2. Incorporation effects of different PNDs at 0.7 wt % on the (a) power efficiency, (b) current density, and (c) luminance of a blue device composed of a 125 nm ITO anode layer, a 35 nm PEDOT:PSS hole-injection layer, a 35 nm solution-processed blue emissive layer of 16 wt % bis[3,5-difluoro-2-(2-pyridyl)phenyl]-(2-carboxypyridyl)iridium(III) (FIrpic) doped in a molecular host of 4,4′-bis(carbazol-9-yl)biphenyl (CBP), a 32 nm 1,3,5-tris(*N*-phenylbenzimidazol-2-yl)benzene electron transport layer, a 0.7 nm lithium fluoride layer, and a 150 nm aluminum cathode layer: Devices with (○) Am-PND, (▽) V-PND, (□) Al-PND, (△) H-PND, and (◇) without PND. Note that the best power efficiency (24.6 lm W^{-1}), found in the H-PND-added device in panel a, was obtained at its optimized concentration of 7 wt %; its efficiency was 20.1 lm W^{-1} at 0.7 wt %.

ation of the R−Si−O−Si bonding group. It is well-known that the alkene group reacts with the hydroxyl group, giving V-PND a negative potential.

It is generally reported that the side-chain density of self-assembled monolayers deposited on oxidized Si through a siloxane network is 5.5 chain nm^{-2}.[31,32] The packing of molecules on oxidized Si is analogous to the modified PND; therefore, if well-ordered side chains formed on the PND, the side-chain density is expected to be approximately 5.5 chain nm^{-2}. On the basis of the average chemical composition of the modified PND and its particle size, the side-chain densities of Am-PND and V-PND are estimated to be 5.3 and 6.0 chain nm^{-2}, respectively. The similarity between the side-chain density on the PND surface and on the amorphous silicon dioxide (SiO_2) surface indicated the complete coverage of functional groups on the PND. On the other hand, the side-chain density of Al-PND is 2.3 group nm^{-2}, indicating that not all of the available sites are occupied on the PND surface. Such a result can be attributed to the lower reactivity of long-chain molecules; the folding of long chains occupied some of the binding sites, leading to less surface coverage.

As Am-PND was incorporated into a hole-transporting device consisting of a hole-injection layer of poly(ethylenedioxythiophene):poly(styrene sulfonic acid) (PEDOT:PSS) sandwiched by a high work-function electrode pair with indium tin oxide (ITO) as the anode and gold (Au) as the cathode, the current density observed with this configuration (Figure 1, middle) was the lowest, indicating the flux of holes was reduced to the greatest extent in the device and that Am-PND was the most effective nanodot in hole modulation. This result may be attributed to the high positive charge of Am-PND, which can presumably repel the injection of holes most effectively because of its strong repulsive effect. Consequently, this process resulted in a relatively small hole-transport flux, balancing the injection of hole against that of electron and maximizing the recombination probability, as illustrated in Figure 1 (right). As a result, the efficiency improvement of bis[3,5-difluoro-2-(2-pyridyl)phenyl]-(2-carboxypyridyl)iridium(III) (FIrpic)-doped blue OLED is the most marked (99%) among all of the devices investigated here after incorporating Am-PND (Figure 2a).

Interestingly, negatively charged V-PND also showed markedly high hole-modulation functionality. In contrast to the repulsion found in Am-PND, the highly negatively charged V-PND was able to trap a significant amount of holes, preventing an excess of holes from entering the emissive layer and leading to a similar efficiency improvement effect (Figure 1, right). This result explains why V-PND is also very effective at improving the efficiency; its incorporation improves the same blue device by 67% (Figure 2a).

It is found that the efficiency improvement strongly depends upon the charge intensity of the nanodot. For example, Al-PND exhibited a charge intensity of +10 mV, a value much lower than that of Am-PND (+22 mV), and its incorporation resulted in only a 62% improvement for the same blue device (Figure 2a). In addition, H-PND exhibited a charge intensity of −5 mV, and its efficiency improvement was only 13%.

In addition to the charge intensity, the nanodot incorporation concentration also strongly affected the efficiency. For Am-PND, the resultant efficiency first increased from 18.0 to 32.3 lm W^{-1} at 100 cd m^{-2} as its concentration increased from 0 to 0.35 wt %, peaked at 35.8 lm W^{-1} with a 0.7 wt % concentration, and then decreased to 31.3 lm W^{-1} at 7 wt %.

The optimized concentrations for the V-PND and Al-PND nanodots were also around 0.7 wt %, and their respective power efficiencies were 30.0 and 29.1 lm W^{-1}. For H-PND, a 7 wt % concentration resulted in a corresponding power efficiency of 24.6 lm W^{-1} (Figure 2a). The optimized concentration may be comparatively higher for H-PND due to its much lower charge intensity, which consequently requires a higher concentration of hole-trapping nanodots to sufficiently re-

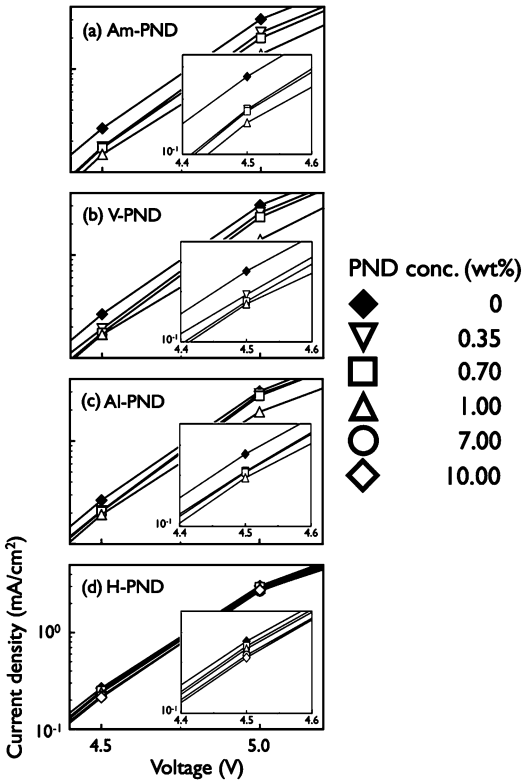

Figure 3. Incorporating concentration effect of different PNDs on the current density of the (a) Am-PND, (b) V-PND, (c) Al-PND, and (d) H-PND blue OLEDs. The incorporation concentration of the PNDs also strongly affected the efficiency. For Am-PND, the resultant current density continuously decreased as the concentration of employed PND increased.

duce the transport flux of holes in order to achieve an optimum carrier recombination.

Figure 2b shows the incorporation effects of nanodots modified with different functional groups on the current density of the blue OLED at 0.7 wt % PND concentration. The measured current density consistently decreased as the charge intensity increased regardless of the charge characters, positive or negative. This trend is in accordance with the device shown in Figure 1; after modification, the charged nanodots are capable of trapping or blocking holes and then modulating the transport flux of holes. This process prevents excessive hole injection into the emissive layer and leads to balanced carrier injection, consequently improving the device efficiency.

Figure 3 shows the incorporating concentration effect on current density for the blue OLEDs containing Am-PND, V-PND, Al-PND, and H-PND. As shown in the figure, all of the current densities decreased as the PND concentration increased, confirming that all of the modified PNDs were effective in hole modulation; however, incorporating an excessive PND concentration led to an over-reduction of the holes entering the emissive layer. This over-reduction causes a reversed hole-deficient and electron-excessive imbalance and, consequently, a poor efficiency.

Figure 2c shows the incorporation effects of nanodots on the luminance of the blue OLED. The device exhibits its brightest emission when Am-PND is incorporated. In addition, the Am-PND-incorporated blue device shows the best power efficiency and the greatest efficiency improvement, as revealed previously. It is important to note that the recombination zone of this device without the incorporation of Am-PND is concentrated at or near the interface of the hole-injection layer and the emissive layer because the interface simultaneously possesses both hole- and electron-blocking functions with blocking barriers of 0.9 and 0.6 eV, respectively. If recombination takes place in a narrow region, excessively populated excitons would be generated in that region, resulting in exciton quenching and a consequent decrease in both luminance and efficiency.[33] Instead, the Am-PND-containing device showed the highest luminance among all those studied, indicating a high recombination probability and a wide recombination region. This result may be attributed to the presence of a high-repulsive field arising from the highly charged Am-PNDs (Figure 1c). Only high-energy holes have a greater probability to pass through the repulsive barriers and thereafter penetrate deeper into the emissive layer. This results in recombination occurring within a wider region—and thus a greater recombination probability—leading to a brighter emission. The same postulation may also apply to the highly negatively charged V-PND device that exhibited relatively high brightness. The only difference here is that the holes entering from the anode must possess high energy to overcome a hole-trapping field that arose from the negative charge of the V-PND (Figure 1, right), rather than a repulsive field, in order to successfully inject into the desired emissive layer.

It is surprising to observe that the Al-PND (+10 mV) device exhibited a higher luminance (14%) than that of the V-PND (−8 mV) counterpart, although their charge intensities are not much different. Generally speaking, the observed luminance increased as the charge intensity increased (based on the same charge character); however, the dependency of luminance on charge intensity was not marked. For the H-PND and V-PND devices, the luminance increased from 76 to 79 cd m^{-2} at 4.5 V, an increase of 4%; their negative charge intensity increased from 5 to 8 mV. Therefore, the marked difference in luminance between the Al-PND and V-PND devices may be attributed to a factor other than charge intensity. The cause is likely related to the charge character, negative or positive. As holes pass through the positively charged nanodots in the Al-PND case, their velocity may increase due to the repulsive force between the holes and the positively charged nanodots, enabling some holes to penetrate deeper into the emissive layer and thus enlarge the recombination area. This process would, in turn, result in a higher luminance. In contrast, the penetration

TABLE 1. Effect of the Emissive Layer Thickness on the Device Power Efficiency with and without PND Incorporation

	power efficiency at 100 cd/m^2 (lm W^{-1})	
emissive layer thickness (nm)	without Am-PND	with Am-PND
43		31
35	18	36
29	20	32
23	22	27
18	23	
14	20	

depth of holes in the emissive layer would be much shorter in the Al-PND case due to the dragging force from the negatively charged nanodots, making the recombination area narrower and resulting in a lower luminance.

Although the penetration depth may further increase as the charge intensity continuously increases, especially in case of positively charged nanodots, it will eventually be limited by the thickness of the emissive layer. This limitation explains why the Am-PND-added device showed a luminance (92 cd m^{-2} at 4.5 V) only slightly higher (2%) than that of the Al-PND counterpart (90 cd m^{-2}) even though the charge intensity was increased from 10 to 22 mV.

Table 1 shows the effect of emissive layer thickness on the device power efficiency with and without PND incorporation. The optimal layer thickness was 18 nm with the highest power efficiency of 23 lm W^{-1} for the device without Am-PND. When Am-PND was incorporated, the optimal layer thickness was 35 nm with a highest power efficiency of 36 lm W^{-1}. The power efficiency was doubled when the Am-PND was incorporated and its corresponding optimal emissive layer thickness was also nearly doubled, confirming that higher power efficiencies can be achieved by having a wider recombination area, as revealed in the literature.[34] This higher efficiency may result from two factors. First, the incorporation of Am-PND effectively blocked excessive holes from entering the emissive layer, leading to a more balanced injection of holes and electrons, as discussed earlier. Second, the highly positively charged Am-PND would allow, most likely, only high energy holes to successfully inject into the emissive layer. This selectivity would cause at least some of the injected holes to penetrate deeper toward the cathode side, resulting in a much wider recombination zone and a much higher power efficiency.

In addition to the blue OLED, Am-PND incorporation was also very effective for OLEDs of other color emissions, including a green OLED containing 12.5 wt % tris(2-phenylpyridine)iridium(III) [Ir(ppy)$_3$], a red OLED containing 3 wt % bis[2-(2′-benzothienyl)pyridinato-N,C$^{3'}$](acetyl acetonate)iridium(III) [(Btp)$_2$Ir(acac)], and a white OLED composed of 0.3 wt % red dye of (Btp)$_2$Ir(acac), 0.08 wt % green dye of Ir(ppy)$_3$, and 14 wt % blue dye of FIrpic. Their respective power efficiency increments were 57, 31, and 54% (Figure 4). It is noteworthy that these results were obtained merely on the basis of the optimized incorporation concentration for the blue device, which was 0.7 wt %. The optimized concentration may be different for other device systems. Much better improvement may be achieved for these three devices if their optimized concentrations are employed.

A preliminary lifetime measurement was carried out for the packaged blue OLEDs with simple encapsulation. Under an initial luminance of 200 cd m^{-2}, the resultant lifetime was increased from 15 ± 1 to 21 ± 2 h, an increase of 40% when Am-PND was added. This finding verifies that the incorporated highly charged nanodot was indeed effective in improving device lifetime. Such an enhancement may be attributed to

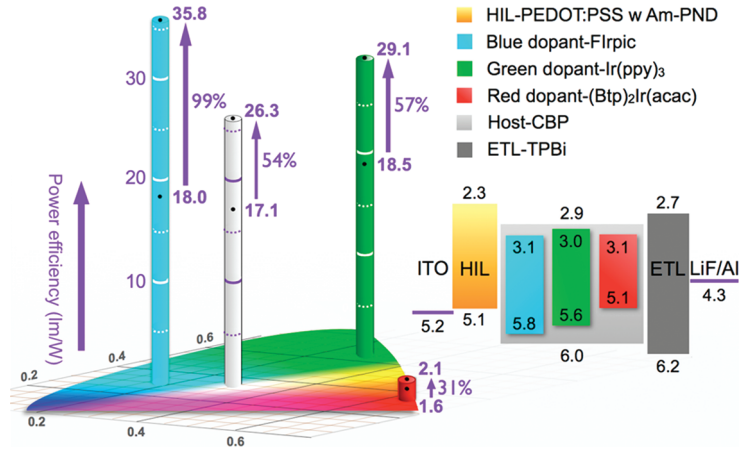

Figure 4. Incorporation effects of Am-PND (0.7 wt %) on the power efficiency of OLED devices with blue, green, red, and white emission; their respective efficiency increments were 99, 57, 31, and 54%. After the incorporation of Am-PND, the blue device showed a two-fold power efficiency improvement over the previous world record. Also shown is the energy level diagram of the devices with different emissive dyes. As demonstrated by the different energy levels exhibited by the different dyes, the optimized PND concentration may vary with varying host/guest combination due to different carrier-trapping characteristics.

the fact that fewer holes were injected into the emissive layer so that damage due to charge accumulation may be reduced. In addition, the resultant higher device efficiency could somewhat reduce heat generated upon emission, preventing damage caused by the generation of excessive heat during operation.[10,33,35] Moreover, as discussed above, the incorporation of Am-PND can enlarge the width of the recombination zone, resulting in an increase in the device lifetime.[33]

CONCLUSIONS

This work demonstrates that the incorporation of highly charged polymeric nanodots with effective carrier modulation functions in the hole-injection layer can substantially advance the efficiency of a high-efficiency blue OLED. Upon the incorporation of the amino-functionalized PND, the resultant power efficiency at 100 cd m^{-2} was increased to nearly 2-fold from an already high 18.0 to a dramatic 35.8 lm W^{-1}. At a high luminance, such as 1000 cd m^{-2}, the efficiency was also enhanced from 12.4 to 21.2 lm W^{-1}, a significant enhancement of 71%. The same method also markedly enhanced the efficiency of other OLED devices with different emissive colors, including white. A substantial advance in power efficiency offers OLEDs the potential to replace current illumination technologies, such as incandescent bulbs and fluorescent tubes, and also offers OLEDs the potential to become a more competitive display because of their better energy-saving, longer stand-by time, and the longer lifetime characteristics.

METHODS

Synthesis and Characterization of Functionalized Polymeric Nanodots: The procedure for preparing H-PND is described below.[36] A solution of 60 g of sodium metasilicate, the H-PND precursor, and 200 mL of deionized water was added to a 200 mL solution of 2.5 M hydrochloric acid while stirring at 0 °C for 5 min. Subsequently, 200 mL of tetrahydrofuran (THF) and 60 g of sodium chloride were sequentially added while stirring for 10 min. After standing for another 10 min, the resultant solution mixture was separated into two layers. The desired organic part (THF) was obtained by leaching out the aqueous solution and was further dried by adding 30 g of anhydrous sodium sulfate. The resultant H-PND-containing solution was left to stand for several hours before the clean upper portion was taken for further experiments. The resultant H-PND was further reacted with 3-aminopropyltriethoxysilane, *n*-octyltrimethoxysilane, and vinyltrimethoxysilane to produce the respective Am-PND, Al-PND, and V-PND. The electrokinetic potential (ζ-potential) of the resultant PNDs was measured using dynamic light scattering measurement (Malvern Zeta Sizer nano-S and Brookhaven zeta-PALS).

Fabrication and Physical Characterization of OLEDs with Functionalized PNDs: The device structure of the OLED consisted with a 125 nm precleaned indium tin oxide (ITO) anode layer on a glass substrate, a 35 nm spin-coated poly(ethylenedioxythiophene):poly(styrene sulfonic acid) (PEDOT:PSS) hole-injection layer (HIL) embedded with the PND, a 35 nm solution-processed blue emissive layer by the use of a premixed solution of 4,4′-bis(carbazol-9-yl)biphenyl (CBP) host and desired guest materials, a 32 nm 1,3,5-tris(*N*-phenylbenzimidazol-2-yl)benzene (TPBi) electron-transporting layer deposited at 2×10^{-5} Torr, a 0.7 nm lithium fluoride layer, and a 150 nm aluminum cathode. For blue, green, and red emission device, the guest consisted of 16 wt % bis[3,5-difluoro-2-(2-pyridyl)phenyl]-(2-carboxypyridyl)iridium(III) (FIrpic), 12.5 wt % tris(2-phenylpyridine)iridium(III) [$Ir(ppy)_3$], and 3 wt % bis[2-(2′-benzothienyl)pyridinato-N,C3′](acetyl acetonate)iridium(III) [$(Btp)_2Ir(acac)$], respectively. The white emission device used a mixed guest of 0.3 wt % red dye of $(Btp)_2Ir(acac)$, 0.08 wt % green dye of $Ir(ppy)_3$ and 14 wt % blue dye of FIrpic.

All of the devices were measured without encapsulation and under ambient conditions. The emissive area of all of the devices was 27 ± 3 mm^2, and only the luminance in the forward direction was measured. The luminance and CIE chromatic coordinates of the resulting OLEDs were measured using a Minolta CS-100A luminance meter. The current−voltage (*I*−*V*) characteristics of the PND-added OLEDs were recorded using a computer-controlled Keithley 2400 electrometer.

Acknowledgment. This work was financially supported under Grant Nos. NCS96-2628-E-007-019-MY3 and NCS95-2221-E-007-128-MY3. We also thank the National Science Council, the National Tsing Hua University, the Academia Sinica, and the Taiwan Semiconductor Manufacturing Company for partial financial support of this work.

REFERENCES AND NOTES

1. Kido, J.; Kimura, M.; Nagai, K. Multilayer White Light-Emitting Organic Electroluminescent Device. *Science* **1995**, *267*, 1332–1334.
2. Duggal, A. R.; Shiang, J. J.; Heller, C. M.; Foust, D. F. Organic Light-Emitting Devices for Illumination Quality White Light. *Appl. Phys. Lett.* **2002**, *80*, 3470–3472.
3. Forrest, S. R. The Road to High Efficiency Organic Light Emitting Devices. *Org. Electron.* **2003**, *4*, 45–48.
4. D'Andrade, B. W.; Forrest, S. R. White Organic Light-Emitting Devices for Solid-State Lighting. *Adv. Mater.* **2004**, *16*, 1585–1595.
5. Burroughes, J. H.; Bradley, D. D. C.; Brown, A. R.; Marks, R. N.; Mackey, K.; Friend, R. H.; Burn, P. L.; Holms, A. B. Light-Emitting-Diodes Based on Conjugated Polymers. *Nature* **1990**, *347*, 539–541.
6. Gustafsson, G.; Cao, Y.; Treacy, G. M.; Klavetter, F.; Colaneri, N.; Heeger, A. J. Flexible Light-Emitting-Diodes Made from Soluble Conducting Polymers. *Nature* **1992**, *357*, 477–479.
7. Jou, J. H.; Sun, M. C.; Chou, H. H.; Li, C. H. White Organic Light-Emitting Devices with a Solution-Processed and Molecular Host-Employed Emission Layer. *Appl. Phys. Lett.* **2005**, *87*, 043508-1–043508-3.
8. Jou, J. H.; Sun, M. C.; Chou, H. H.; Li, C. H. Efficient Pure-White Organic Light-Emitting Diodes with a Solution-Processed, Binary-Host Employing Single Emission Layer. *Appl. Phys. Lett.* **2006**, *88*, 141101-1–141101-3.
9. Ding, J. Q.; Gao, J.; Cheng, Y. X.; Xie, Z. Y.; Wang, L. X.; Ma, D. G.; Jing, X. B.; Wang, F. S. Highly Efficient Green-Emitting Phosphorescent Iridium Dendrimers Based on Carbazole Dendrons. *Adv. Funct. Mater.* **2006**, *16*, 575–581.
10. Jou, J. H.; Chen, C. C.; Chung, Y. C.; Hsu, M. F.; Wu, C. H.; Shen, S. M.; Wu, M. H.; Wang, W. B.; Tsai, Y. C.; Wang, C. P.; *et al.* Nanodot-Enhanced High-Efficiency Pure-White Organic Light-Emitting Diodes with Mixed-Host Structures. *Adv. Funct. Mater.* **2008**, *18*, 121–126.
11. Jou, J. H.; Hsu, M. F.; Wang, W. B.; Liu, C. P.; Wong, Z. C.; Shyue, J. J.; Chiang, C. C. Small Polymeric Nano-Dot Enhanced Pure-White Organic Light-Emitting Diode. *Org. Electron.* **2008**, *9*, 291–295.
12. Caruge, J. M.; Halpert, J. E.; Bulović, V.; Bawendi, M. G. NiO as an Inorganic Hole-Transporting Layer in Quantum-Dot Light-Emitting Devices. *Nano Lett.* **2006**, *6*, 2991–2994.

13. Carter, S. A.; Scott, J. C.; Brock, P. J. Enhanced Luminance in Polymer Composite Light Emitting Devices. *Appl. Phys. Lett.* **1997**, *71*, 1145–1147.
14. Bliznyuk, V.; Ruhstaller, B.; Brock, P. J.; Scherf, U.; Carter, S. A. Self-Assembled Nanocomposite Polymer Light-Emitting Diodes with Improved Efficiency and Luminance. *Adv. Mater.* **1999**, *11*, 1257–1261.
15. Kim, Y. K.; Lee, K. Y.; Kwon, O. K.; Shin, D. M.; Sohn, B. C.; Choi, J. H. Size Dependence of Electroluminescence of Nanoparticle (Rutile-TiO_2) Dispersed MEH-PPV Films. *Synth. Met.* **2000**, *111*, 207–211.
16. Oey, C. C.; Djurišić, A. B.; Kwong, C. Y.; Cheung, C. H.; Chan, W. K.; Nunzi, J. M.; Chui, P. C. Nanocomposite Hole Injection Layer for Organic Device Applications. *Thin Solid Films* **2005**, *492*, 253–258.
17. Zhang, Z. F.; Deng, Z. B.; Liang, C. J.; Zhang, M. X.; Xu, D. H. Organic Light-Emitting Diodes with a Nanostructured TiO_2 Layer at the Interface between ITO and NPB Layers. *Displays* **2003**, *24*, 231–234.
18. Shih, P. I.; Chien, C. H.; Wu, F. I.; Shu, C. F. A Novel Fluorene-Triphenylamine Hybrid That Is a Highly Efficient Host Material for Blue-, Green-, and Red-Light-Emitting Electrophosphorescent Devices. *Adv. Funct. Mater.* **2007**, *17*, 3514–3520.
19. Deng, Z. B.; Ding, X. M.; Lee, S. T.; Gambling, W. A. Enhanced Brightness and Efficiency in Organic Electroluminescent Devices Using SiO_2 Buffer Layers. *Appl. Phys. Lett.* **1999**, *74*, 2227–2229.
20. Poon, C. O.; Wong, F. L.; Tong, S. W.; Zhang, R. Q.; Lee, C. S.; Lee, S. T. Improved Performance and Stability of Organic Light-Emitting Devices with Silicon Oxy-Nitride Buffer Layer. *Appl. Phys. Lett.* **2003**, *83*, 1038–1040.
21. Zhu, F. R.; Low, B. L.; Zhang, K. R.; Chua, S. J. Lithium-Fluoride-Modified Indium Tin Oxide Anode for Enhanced Carrier Injection in Phenyl-Substituted Polymer Electroluminescent Devices. *Appl. Phys. Lett.* **2001**, *79*, 1205–1207.
22. Xie, Z. Y.; Hung, L. S.; Lee, S. T. High-Efficiency Red Electroluminescence from a Narrow Recombination Zone Confined by an Organic Double Heterostructure. *Appl. Phys. Lett.* **2001**, *79*, 1048–1050.
23. Hung, L. S.; Chen, C. H. Recent Progress of Molecular Organic Electroluminescent Materials and Devices. *Mater. Sci. Eng. R* **2002**, *39*, 143–222.
24. Jou, J. H.; Chiu, Y. S.; Wang, C. P.; Wang, R. Y.; Hu, H. C. Efficient, Color-Stable Fluorescent White Organic Lght-Emitting Diodes with Single Emission Layer by Vapor Deposition from Solvent Premixed Deposition Source. *Appl. Phys. Lett.* **2006**, *88*, 193501-1–193501-3.
25. Jou, J. H.; Wang, C. J.; Lin, Y. P.; Chung, Y. C.; Chiang, P. H.; Wu, M. H.; Wang, C. P.; Lai, C. L.; Chang, C. Color-Stable, Efficient Fluorescent Pure-White Organic Light-Emitting Diodes with Device Architecture Preventing Excessive Exciton Formation on Guest. *Appl. Phys. Lett.* **2008**, *92*, 223504-1–223504-3.
26. Lee, M. T.; Liao, C. H.; Tsai, C. H.; Chen, C. H. Highly Efficient, Deep-Blue Doped Organic Light-Emitting Devices. *Adv. Mater.* **2005**, *17*, 2493–2497.
27. Adamovich, V. I.; Cordero, S. R.; Djurovich, P. I.; Tamayo, A.; Thompson, M. E.; D'Andrade, B. W.; Forrest, S. R. New Charge-Carrier Blocking Materials for High Efficiency OLEDs. *Org. Electron.* **2003**, *4*, 77–87.
28. Jou, J. H.; Hsu, M. F.; Wang, W. B.; Chin, C. L.; Chen, S. Z.; Chen, C. T.; Chung, Y. C.; Chen, C. C.; Liu, C. P.; Wang, C. J.; *et al.* Solution-Processable, High-Molecule-Based Trifluoromethyl-Iridium Complex for Extraordinarily High Efficiency Blue-Green Organic Light-Emitting Diode. *Chem. Mater.* **2009**, *21*, 2565–2567.
29. Jou, J. H.; Lin, Y. P.; Hsu, M. F.; Wu, M. H.; Lu, P. High Efficiency Deep-Blue Organic Light-Emitting Diode with a Blue Dye in Low-Polarity Host. *Appl. Phys. Lett.* **2008**, *92*, 193314-1–193314-3.
30. Namai, H.; Ikeda, H.; Hoshi, Y.; Kato, N.; Morishita, Y.; Mizuno, K. Thermoluminescence and a New Organic Light-Emitting Diode (OLED) Based on Triplet-Triplet Fluorescence of the Trimethylenemethane (TMM) Biradical. *J. Am. Chem. Soc.* **2007**, *129*, 9032–9036.
31. Shyue, J. J.; Tang, Y.; De Guire, M. R. Forces between Nitrogen-Containing Self-Assembled Monolayers (SAMs) and Zirconia Particles in Aqueous Solutions. *J. Mater. Chem.* **2005**, *15*, 323–330.
32. Shin, H.; Agarwal, M.; De Guire, M. R.; Heuer, A. H. Deposition Mechanism of Oxide Thin Films on Self-Assembled Organic Monolayers. *Acta Mater.* **1998**, *46*, 801–815.
33. Tsai, Y. C.; Jou, J. H. Long-Lifetime, High-Efficiency White Organic Light-Emitting Diodes with Mixed Host Composing Double Emission Layers. *Appl. Phys. Lett.* **2006**, *89*, 243521-1–243521-3.
34. Zhang, X.; Wei, F.; Liu, X.; Zhu, W.; Jiang, X.; Zhang, Z. Obtaining High-Efficiency Red Electrophosphorescent OLEDs by Changing the Thickness of Light-Emitting Layer. *Displays* **2007**, *28*, 150–153.
35. Aziz, H.; Popvic, Z. D. Degradation Phenomena in Small-Molecule Organic Light-Emitting Devices. *Chem. Mater.* **2004**, *16*, 4522–4532.
36. Hsu, Y. G.; Lin, K. H.; Chiang, I. L. Organic−Inorganic Hybrid Materials Based on the Incorporation of Nanoparticles of Polysilicic Acid with Organic Polymers. 1. Properties of the Hybrids Prepared through the Combination of Hydroxyl-Containing Linear Polyester and Polysilicic Acid. *Mater. Sci. Eng., B* **2001**, *87*, 31–39.